Journal of Applied Electrochemistry **32**: 701–707, 2002.
© 2002 *Kluwer Academic Publishers. Printed in the Netherlands.*

Influence of copper anion complexes on the incorporation of metal particles in polyaniline
Part I: Copper citrate complex

S. IVANOV and V. TSAKOVA*
Institute of Physical Chemistry, Bulgarian Academy of Sciences, Bg-1113 Sofia, Bulgaria
*(*author for correspondence, fax: +359 2 9712688, e-mail: tsakova@ipchp.ipc.bas.bg)*

Received 11 December 2001; accepted in revised form 4 April 2002

Key words: citrate metal complex, copper electrodeposition, microcrystals, polyaniline

Abstract

Copper electrodeposition in polyaniline-coated electrodes is studied using copper citrate complex anions as reducing species. Use of these complex anions allows shifting the potential window for metal deposition in the negative direction and resolving the polymer and metal reduction processes. As shown by galvanostatic experiments and SEM photographs, copper electrodeposition from citrate solution is highly inhibited and results in a small number (3.6×10^6 cm^{-2}) of large hemispherical crystals located mainly on top of the polymer layer. Statistical analysis of distances between neighbouring crystals shows a random surface distribution of the copper hemispheres. Thus, the low number of crystals obtained cannot be related to the appearance and overlap of nucleation exclusion zones partly blocking the electrode surface. It is likely connected to the specific role of the metal anion complexes in the deposition process and more precisely to the inhibited diffusion of both the copper complex anions and the released (after reduction) citrate anions in and out of the polymer structure.

1. Introduction

In recent years metal deposition in conducting polymer layers has been intensively studied due to the interest in producing metal/polymer composites for various purposes. Most studies in the field are devoted to the deposition of the catalytic metals platinum, palladium and gold [1–4]. Although not of such general interest, metals like silver, nickel and copper have also been the subject of several studies [5–17]. Most of these studies have aimed at determining whether each specific metal/polymer composite exhibits special (i.e., catalytic, gas sensing etc.) properties. A few attempts [3, 4, 8, 9, 15–17] were made to reveal the influence of different factors such as polymerization or metal deposition procedures on the location, number and size of deposited metal particles.

In previous investigations [15–17] on copper deposition in polyaniline we have demonstrated the role of polymer layer thickness [15] and polymer synthesis conditions [16] with respect to the number and size distribution of the deposited crystals. A detailed study on the kinetics of copper nucleation and growth was performed [17]. In these investigations copper deposition occurred from an acid copper sulfate solution, copper cations being the species reduced. The aim of the present study is to explore the effect of copper anion complexes as the source for metal reduction on the deposition kinetics and the number and size of deposited copper crystals. As is well known, the involvement of metal anion complexes in electrocrystallization allows shifting of the deposition potential in the negative direction. This effect is of special interest when using conducting polymer modified electrodes. Indeed, the oxidation state and, thus, the conductivity of the polymer layer depends on potential. Thus shifting the metal deposition potential window allows, in principle, working at different oxidation states of the polymer layers. Another specific effect, which might arise by using metal ion complexes for electrodeposition in conducting polymer layers, relates to the transport of the metal-containing species through the polymer structure. It may be expected that, depending on the size of the complexing ligands, a size selective transport could occur in the polymer porous structure. This would possibly allow the number and size of the deposited metal crystals to be influenced. Beside these specific effects connected to the characteristics of the polymer layers alone, metal ion complexes can, in principle, influence the growth and, eventually, the morphology of the metal crystals.

The main objective of this study is to explore the possible incidence of the effects already mentioned above in the copper/polyaniline system. Two different copper anion complexes, copper citrate and copper oxalate,

were used for metal deposition. The first part of this study presents the results obtained with copper citrate complex used as reducing species. In the second part we present an investigation of metal deposition from copper oxalate solution and the comparison is made between results obtained with both copper anion complexes.

2. Experimental details

The electrochemical cells used in all experiments consisted of a platinum single crystal(bead) working electrode with surface area $S = 2.3 \times 10^{-3}$ cm^2, a mercury sulfate reference electrode (MSE) and a platinum plate counter electrode. All potentials in the text are given with respect to the MSE. In the acid solutions a Hg/Hg_2SO_4/0.5 M H_2SO_4 electrode with $E_{MSE} = 0.68$ V vs SHE was used. In the copper plating solution a Hg/Hg_2SO_4/0.5 M K_2SO_4 with $E_{MSE} = 0.66$ V vs SHE was employed.

Polyaniline (PAN) layers were synthesized in an aqueous solution of 0.1 M aniline and 0.5 M H_2SO_4 by means of a pulse potentiostatic procedure [18, 19]. The latter allows formation of homogeneous polymer layers with low amount of macrodefects [16]. The parameters of the anodic and cathodic pulses used for polymerization were $E_a = 0.322$ V, $t_a = 0.1$ s and $E_c = -0.48$ V, $t_c = 0.1$ s, respectively. The thickness of the polymer layers was varied by changing the number of pulse cycles.

After polymerization, the polymer-coated electrode was transferred in an electrochemical cell containing supporting electrolyte (0.5 M H_2SO_4) for measuring the redox activity of the deposited layer. The reduction charge, Q_{red}^{PAN}, of PAN was determined by scanning the potential within potential limits −0.64 and 0.32 V at 100 mV s^{-1}. Q_{red}^{PAN} is an indirect measure for the polymer layer thickness. Complete reduction of the PAN layers, necessary in some sets of experiments, was also performed by holding the potential at −0.64 V for 15 min in this solution.

The copper deposition occurred galvanostatically in an aqueous solution of 0.02 M $CuSO_4$, 0.062 M $K_3C_6H_5O_7$ and 0.344 M K_2SO_4 at pH 6.06. As is well known, at this pH value the citrate complex $[Cu\text{-}C_6H_5O_7]^-$ (denoted further as CuCit) is formed [20]. The equilibrium potential of copper in this solution was measured to be $E_0^{Cu} = -0.565$ V vs MSE. According to the literature [21], the stability constant of the CuCit complex is $\log K_1 = 5.9$. One water molecule per CuCit complex takes part in the ligand shell of the complex ion [22] as in Structure 1.

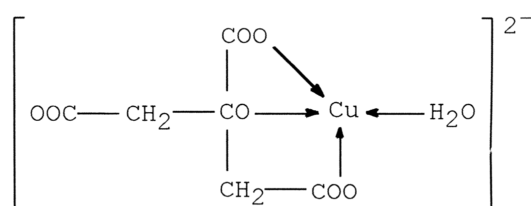

Structure 1.

All galvanostatic deposition experiments were performed with a current density $i = -0.18$ mA cm^{-2}.

Oxidation curves were measured after each copper deposition at a slow sweep rate (5 mV s^{-1}) in positive direction. To obtain the charge related to the copper oxidation alone, the oxidation curve of the PAN layer itself (registered for each layer after PAN synthesis) was subtracted from the oxidation curve measured after metal deposition. The curves resulting after the subtraction are denoted in the text as copper oxidation curves.

Cu/PAN specimens for SEM were prepared using platinum plate electrodes of surface area 1 cm^2. The imaging was performed on a JSM 5300 (Jeol) microscope. SEM micrographs were used for statistical analysis of the distances between the closest crystals. Computations were performed by means of a home-made program.

3. Results and discussion

As described in the experimental part, after synthesis and characterization in acid solutions, for the next step of metal deposition PAN layers were transferred to a nearly neutral solution at pH 6.06. It is well known that PAN loses its redox activity at pH values higher than 4 [23, 24]. However, the exchange of the electrolyte inside the film takes place only after several potentiodynamic cycles [24] and the first cycle of an oxidized PAN layer transferred from acid to nearly neutral solution exhibits a marked reduction peak. Figure 1 shows first scans measured on PAN coated electrodes in three different solutions at about the same pH value: K_2SO_4 alone, supporting electrolyte consisting of both K_2SO_4 and KCit and the CuCit containing solution itself. It is evident that the potential position of the reduction peak depends strongly on the solution anion composition and that in the presence of citrate anions polymer layer reduction occurs more easily. It is worth noting here that in the case of copper deposition from an acid copper sulfate solution, the potential windows for PAN layer reduction and metal deposition overlap and for this reason copper deposition depends significantly on the initial oxidation state of the polymer layers [16]. As seen in Figure 1, in the present case metal and polymer reduction processes seem to be completely resolved and for this reason metal deposition should hardly depend on the initial oxidation state of PAN. Indeed, the potential curves measured at constant cathodic current at an oxidized and a reduced (prior to the transfer in the copper ion containing cell) PAN layer show similar behaviour for $E < E_0^{Cu}$ (Figure 2). Of course, the oxidized PAN coated electrode undergoes reduction first, which is fully completed before the copper equilibrium potential in this solution is reached.

The potential transients (Figure 2) show that high negative potentials are needed for initiating the copper deposition reaction. No typical nucleation and growth maxima are observed. This should mean that metal

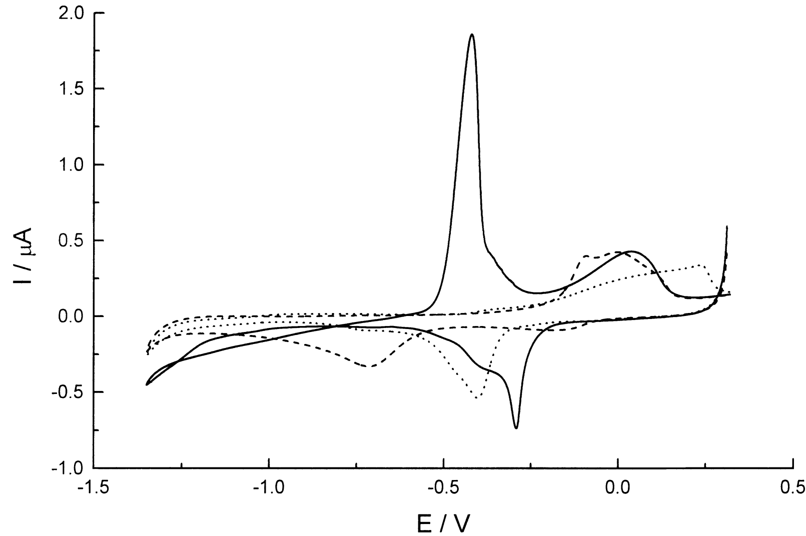

Fig. 1. Potentiodynamic curves measured at a PAN coated electrode ($Q_{red}^{PAN} = 5$ mC cm^{-2}) in the copper citrate solution (—), in 0.344 M K_2SO_4 + 0.062 K_3Cit (···) and in 0.344 M K_2SO_4 (- - -) solutions.

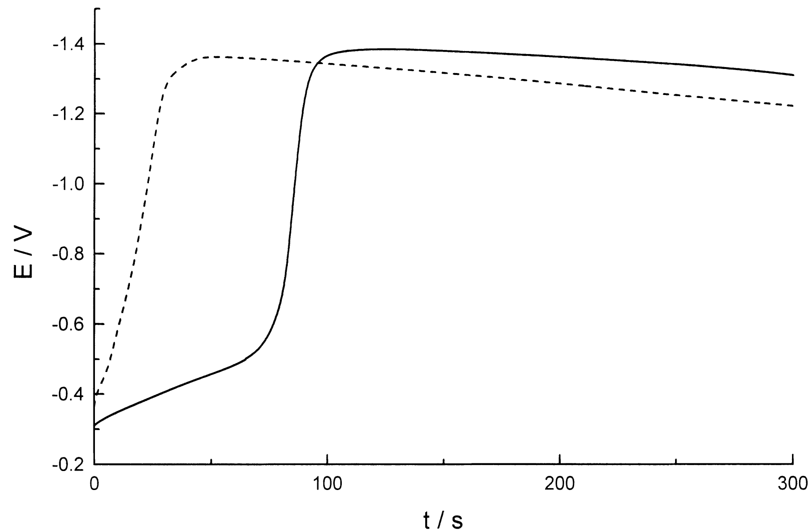

Fig. 2. Galvanostatic copper deposition curves measured at oxidized (—) and reduced (- - -) PAN coated electrodes. $Q_{red}^{PAN} = 20$ mC cm^{-2}. (Reduction of the PAN layer occurred in acid 0.5 M H_2SO_4 solution.)

nucleation and growth are highly inhibited at least at this thickness of polymer coating. A series of galvanostatic experiments, performed on PAN coated electrodes with different reduction charges ranging from 1.7 to 20 mC cm^{-2} (Figure 3), show that both the potential window for metal deposition and the shape of the galvanostatic curve depend significantly on the polymer layer thickness. Galvanostatic curves exhibiting maxima and low overpotentials for deposition are found on thin PAN layers, whereas the thicker ones require high negative potentials reaching the hydrogen reduction potential (dotted lines in Figure 3). However, very thin PAN layers are expected to be nonhomogeneous and to possess a number of macrodefect regions. Only thicker ones are really suitable for dispersing of a large number of small metal inclusions [15, 17]. Obviously, at thick PAN layers, at least in the initial stage, hydrogen reduction and metal deposition occur in parallel in the copper citrate solution and both determine the overall behaviour of the potentiostatic curve.

Further information about the electrodeposited copper species was obtained by measuring slow potentiodynamic oxidation curves after the galvanostatic copper deposition. The oxidation curve of the PAN layer alone, measured after synthesis of each layer, was subtracted from the corresponding copper oxidation curve. Figure 4 shows the resulting data for both oxidized and reduced PAN specimens used in the electrodeposition experiment already shown (Figure 2). There are two well-resolved copper dissolution peaks in both cases: the first, more negative one, should correspond to copper species easily released from the electrode surface. As for the second, more positive oxidation peak, it overlaps the potential region where PAN itself oxidizes and a

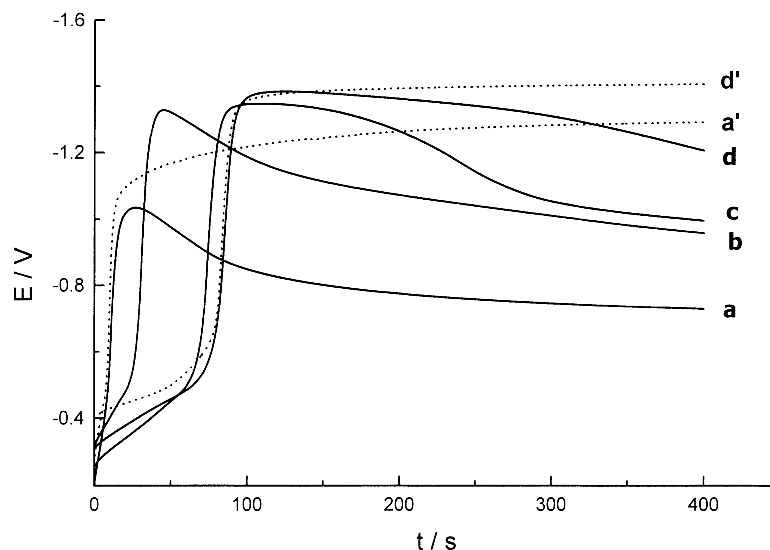

Fig. 3. Galvanostatic copper deposition curves measured at oxidized PAN coated electrodes with different Q_{red}^{PAN}: (a) 1.7, (b) 6.1, (c) 11.3, and (d) 20 mC cm^{-2}. Dashed lines denote galvanostatic curves measured in supporting electrolyte (K_2SO_4 + K_3Cit) at two of the PAN layers.

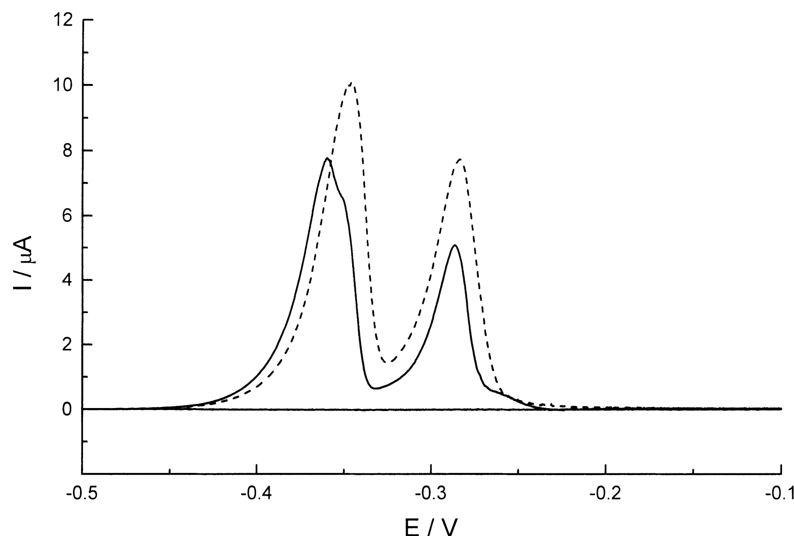

Fig. 4. Copper oxidation curves registered after galvanostatic deposition at the oxidized (—) and reduced (- - -) PAN coated electrodes (see Figure 2).

nonconducting to conducting state transition takes place. This means that copper deposit corresponding to the second oxidation peak can be released only after the polymer layer has been driven in its conducting state thus making the electronic contact with these copper species possible.

To understand the origin of both dissolution peaks, and thus of both types of deposited copper species, a series of experiments at different duration of galvanostatic deposition were performed at PAN layers having the same thickness. It was found (Figure 5) that the second more positive peak arises first and remains dominant up to copper loadings of about 10 mC cm^{-2}. Then, with increasing copper deposition charge, the first peak of copper oxidation gradually exceeds the second one, both peaks continuing to grow. Having in mind that the copper electrodeposition starts in a completely reduced, nonconducting polymer layer, it may be assumed that metallic paths are formed through the layer first, before the emerging of copper crystals on the surface becomes possible. Copper crystals could not be detected at the polymer surface for small amounts of deposited copper (<10 mC cm^{-2}). Thus, the initial occurrence and growth of the second oxidation peak should be connected to copper species incorporated in the polymer layer. The appearance of the first dissolution peak after a certain of deposition charge has been exceeded should be related to copper emerging at the polymer–electrolyte interface and growing outside the polymer layer. If this is so, it seems surprising that the second oxidation peak does not come to a saturation and continues growing even for large amounts of deposited copper.

To clarify this problem, copper was galvanostatically deposited in the same manner at two PAN coated

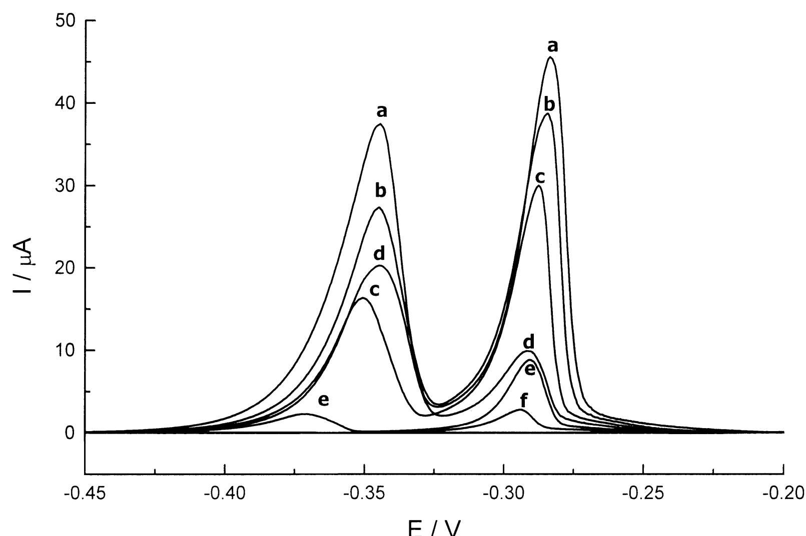

Fig. 5. Copper oxidation curves registered after galvanostatic deposition for different times: (a) 1400, (b) 1100, (c) 800, (d) 700, (e) 400 and (f) 310 s.

platinum plate electrodes. One of the two specimens was directly used for scanning electron microscopy. The second was first subjected to a partial oxidation at −0.4 V for 300 s and then explored by SEM. Micrographs of typical individual copper crystals from both specimens are presented in Figure 6. In contrast to the well-shaped hemispherical crystal seen at the 'as grown' specimen, the partially oxidized specimen shows partly dissolved crystals exhibiting a rough cauliflower structure. To relate the copper structures seen at the micrographs to the electrochemical oxidation behaviour, the experiments described above were repeated by performing (after the deposition or after the hold time, respectively) a slow positive potential sweep (Figure 7). As can be seen from the electrochemical measurements, the charge under the second dissolution peak corresponds to the partially dissolved metallic crystals. Obviously, during the first step of copper dissolution, which should occur through the conducting metallic paths existing in the polymer layer, a considerable amount of copper loses electronic contact with the underlying metal surface and remains intact on the polymer surface. Release becomes possible only after the electronic conductivity of PAN has been regained.

The micrographs allow estimation of the average number of copper crystals deposited from the copper citrate solution. It was found to be 3.6×10^6 cm^{-2} and thus about two orders of magnitude smaller then the number of copper crystals deposited from acid copper sulfate solution at PAN layers with the same thickness [16, 17]. Having in mind the large average size of the copper crystals obtained in the present experiments, it can be assumed that the appearance of nucleation exclusion zones is the reason for the low number of deposited crystals. Indeed, the gradual spreading of zones of reduced overpotential around each growing crystal might inhibit further nucleation and reduce the total number of metal crystals. To verify this

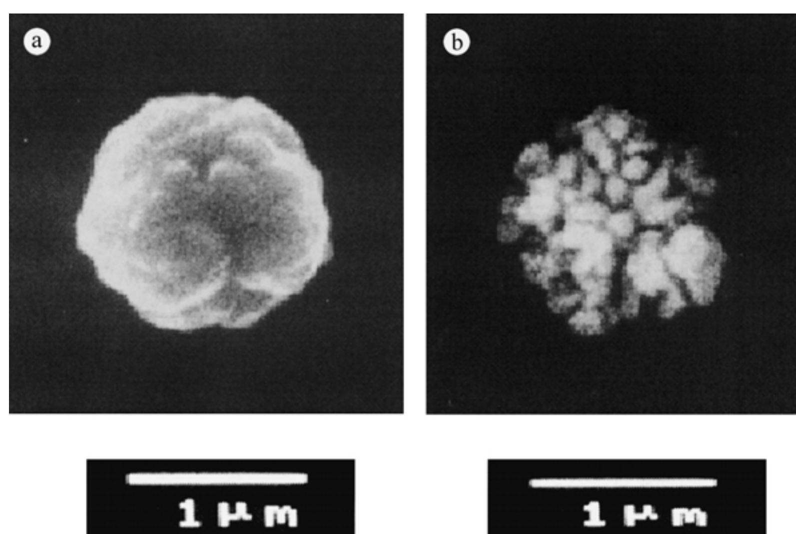

Fig. 6. SEMs of individual crystals after deposition (a) and after partial dissolution (b).

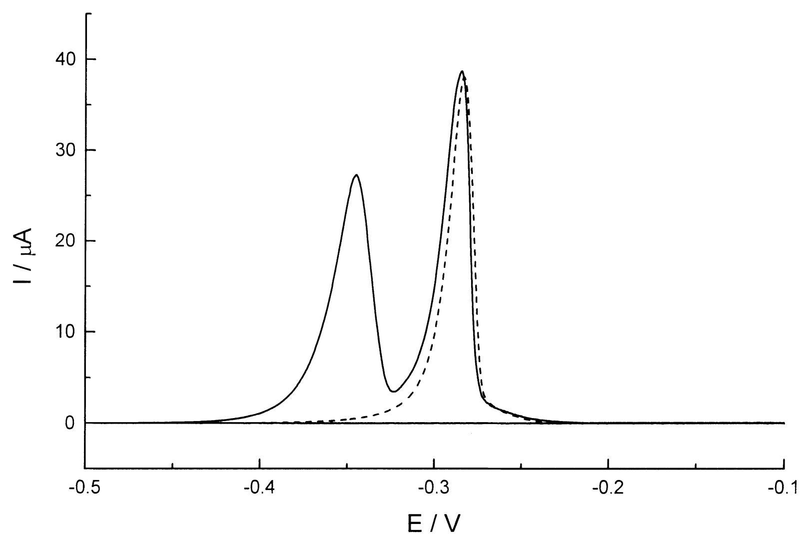

Fig. 7. Copper oxidation curves obtained after galvanostatic deposition at two PAN coated electrodes ($Q_{red}^{PAN} = 20$ mC cm^{-2}). Full line obtained directly after deposition. Dashed line obtained after potential hold at $E = -0.4$ V for 300 s.

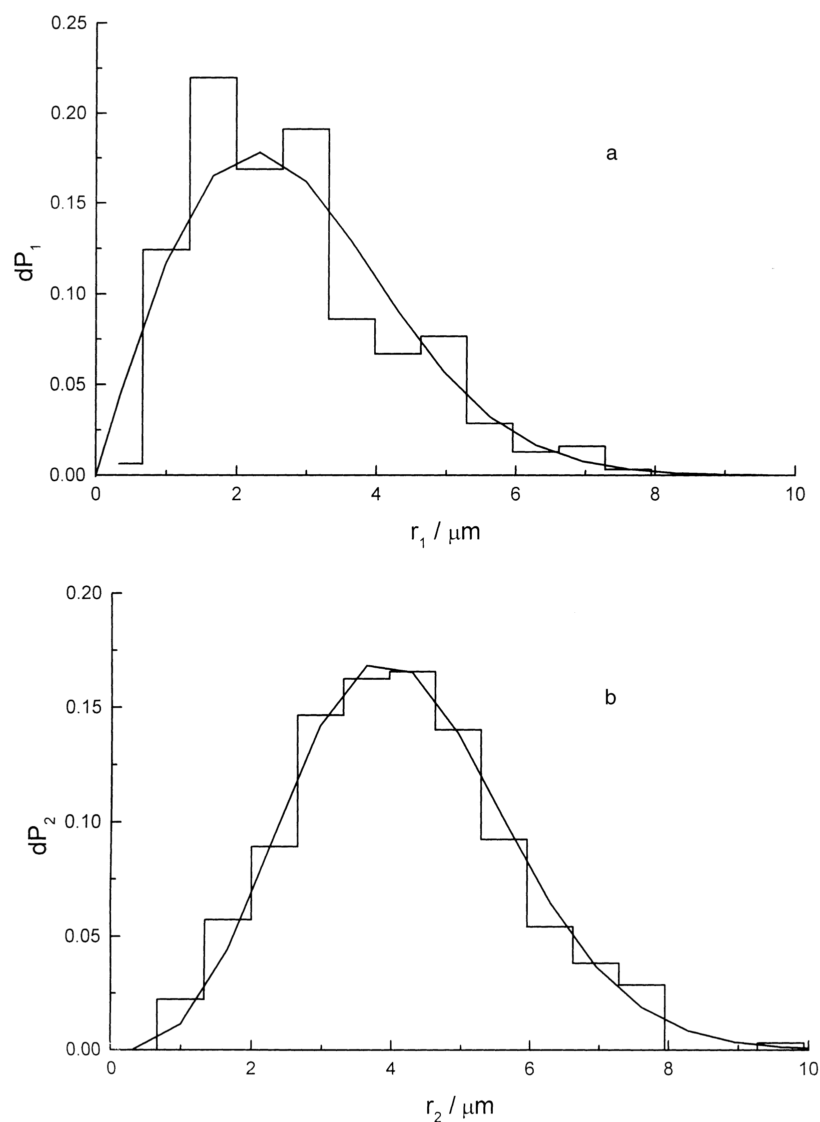

Fig. 8. Experimental (histograms) and Poissonian (full lines) distributions of the distances between the first (a) and the second (b) neighbouring crystals. (Copper crystals deposited galvanostatically at PAN coated electrode with $Q_{red}^{PAN} = 20$ mC cm^{-2}.)

assumption, a statistical analysis [25, 26] of the distances between the first and the second neighbouring crystals was performed and compared to the theoretical distance distributions corresponding to a random Poissonian process. A deviation from the theoretical prediction might be expected in the case of a marked influence of nucleation exclusion zones. Figure 8 shows the experimental histograms and the theoretical lines for the first and second neighbouring crystals. In both cases the experimental distributions correspond to Poissonian. This means that the zones of reduced overpotential do not influence the nucleation and growth process and are not a reason for the low number of deposited crystals.

4. Conclusions

The use of copper citrate anion complexes allows shifting of the potential window for metal deposition in the negative direction and thus completely resolving the polymer and metal reduction processes. As a consequence, the initial oxidation state of the polyaniline layer no longer plays a crucial role in the metal deposition, as in the case of copper cation reduction [16]. However, the copper nucleation and growth occurring in the citrate solution turn out to be strongly inhibited as high overpotentials are needed for the deposition of a low number of copper crystals. As estimated from the charge under the second oxidation peak (before the emerging of the first one), the amount of copper incorporated in the layer is limited. Growth occurs preferentially on top of the polymer surface. The number of copper crystals obtained is two orders of magnitude smaller than the number of copper crystals obtained in the Cu^{2+} reduction case. As shown by the statistical analysis of the distances between neighbouring crystals, the small number density of crystals is not related to the specific effects of the spreading and overlap of nucleation exclusion zones. Thus, other factors play a decisive role in the inhibition of the electrodeposition process.

One possibility is to assume that copper citrate complexes have high stability and that large negative potentials are needed for copper reduction. The large citrate anions also have to diffuse out after reduction and the transport of both complex copper ions inside the layer and citrate anions out of the polymer layer has to occur through a complex porous medium. Indeed, it is known that PAN has a porous structure with large pore size distribution ranging between 1 and 100 nm [27]. It may be assumed that copper citrate complexes and citrate anions diffuse only through the larger pores of the polymer structure and this is the limiting factor for obtaining small quantities of copper deposited in the reduced and compressed polymer.

In any case metal deposition should be very sensitive to the size and stability of the complex metal ion used for metal reduction. To explore this point further, investigations on copper deposition on PAN using copper oxalate as reducing agent were performed in the second part of this work [28].

Acknowledgements

The authors thank Prof. D. Stoychev for fruitful discussions and B. Ranguelov for kind cooperation in obtaining SEM pictures of Cu/PAN specimens. The investigations were completed with the financial support of the Bulgarian Ministry of Science and Education under contract X-1008. The equipment used in all electrochemical experiments was a donation (to V.T.) by the Alexander von Humboldt Foundation, Germany.

References

1. A. Malinauskas, *Synthetic Metals* **107** (1999) 75.
2. M. Musiani, *Electrochim. Acta* **45** (2000) 3397.
3. K. Bouzek, K-M. Mangold and K. Jüttner, *Electrochim. Acta* **46** (2000) 661.
4. V. Tsakova, S. Winkels and J.W. Schultze, *J. Electroanal. Chem.* **500** (2001) 574.
5. Z.Q. Tian, Y.Z. Lian, J.Q. Wang, S.J. Wang and W.H. Li, *J. Electroanal. Chem.* **308** (1991) 357.
6. V. Tsakova and A. Milchev, *Electrochim. Acta* **36** (1991), 1151.
7. A.Q. Zhang, C.Q. Cui, J.Y. Lee and F.C. Loh, *J. Electrochim. Soc.* **l42** (1995) 1097.
8. L.M. Abrantes and J.P. Correia, *Surf. Coat. Technol.* **107** (1998) 142.
9. L.M. Abrantes and J.P. Correia, Portug. *Electrochim. Acta* **16** (1998) 85.
10. L.M. Abrantes and J.P. Correia, *Electrochim. Acta* **45** (2000) 4179.
11. M. Hepel, Y-M. Chen and R. Stephenson, *J. Electrochem. Soc.* **143** (1996) 498.
12. A. Zouaoui, O. Stephan, M. Carrier and J-C. Moutet, *J. Electroanal. Chem.* **474** (1999) 113.
13. R.J. Nichols, D. Schröer and H. Meyer, *Electrochim. Acta* **40** (1995) 1479.
14. J.M. Ortega, *Thin Solid Films* **360** (2000), 159.
15. V. Tsakova and D. Borissov, *Electrochem. Commun.* **2** (2000) 511.
16. V. Tsakova, D. Borissov and S. Ivanov, *Electrochem. Commun.* **3** (2001) 312.
17. V. Tsakova, D. Borissov, B. Ranguelov, Ch. Stromberg and J.W. Schultze, *Electrochim. Acta* **46** (2001) 4213.
18. V. Tsakova and A. Milchev, *Electrochim. Acta* **36** (1991) 1579.
19. V. Tsakova, A. Milchev and J.W. Schultze, *J. Electroanal. Chem.* **346** (1993) 85.
20. H. Natter and R. Hempelmann, *J. Phys. Chem.* **100** (1996) 19525.
21. A.E. Martell and R.M. Smith, Critical Stability Constants, Vols. 1–3 (Plenum, New York, 1977).
22. Gmelin's 'Handbuch der Anorganischen Chemie', Bd.60, T1.B, Lfg.2, Springer Verlag, Berlin, 1966, pp. 798–799.
23. W.-S. Huang, B. Humphrey and A.G. Macdiarmid, *J. Chem. Soc., Faraday Trans. 1*, **82** (1986) 2385.
24. G. Inzelt and G. Horanyi, *Electrochim. Acta* **35** (1990) 27.
25. A. Milchev, *J. Chem. Phys.* **100** (1994) 5160.
26. V. Tsakova and A. Milchev, *J. Electroanal. Chem.* **451** (1998) 211.
27. Yu. M. Volfkovich, A.G. Sergeev, T.K. Zolotova, S.D. Afanasiev, O.N. Efimov and E.P. Krinichnaya, *Electrochim. Acta* **44** (1999) 1543.
28. S. Ivanov and V. Tsakova, *J. Appl. Electrochem.*, this issue.